Low-Complexity Channel Estimation for OFDM and MC-CDMA

J. Akhtman and L. Hanzo

School of ECS., Univ. of Southampton, SO17 1BJ, UK.
Tel: +44-23-80-593 125, Fax: +44-23-80-593 045
Email: lh@ecs.soton.ac.uk, http://www-mobile.ecs.soton.ac.uk

Abstract— A low complexity decision-directed channel estimation method is proposed, which is suitable for a wide range of multi-carrier modulation schemes such as OFDM and MC-CDMA. The method exploits the *a priori* knowledge available concerning the nature of the wireless channel and exploits both the time- and frequency-domain correlation of the channel parameters, yet it is shown to be robust to the channel model mismatch routinely encountered in practical propagation environments. The performance of the OFDM system using the channel estimation scheme proposed in the scenario of encountering multipath Rayleigh-fading channel conditions is shown to be close to that of the idealistic system assuming perfect channel knowledge.

I. INTRODUCTION

The ever-increasing demand for high data-rates in wireless networks requires the efficient utilisation of the limited bandwidth available, while supporting a high grade of mobility in diverse propagation environments. Orthogonal Frequency Devision Multiplexing (OFDM) and Multi-Carrier Code Devision Multiple Access (MC-CDMA) techniques [1] are capable of satisfying these requirements. This is a benefit of their ability to cope with highly time-variant wireless channel characteristics. However, as pointed out in [2], the capacity and the achievable integrity of communication systems is highly dependent on the system's knowledge concerning the channel conditions encountered. Thus, the provision of an accurate and robust channel estimation strategy is a crucial factor in achieving a high performance.

The rest of this paper is structured as follows. The system model and the channel model considered are described in Section II. A one-dimensional *a posteriori* decision directed channel estimator is derived in Section III-A. The resultant one-dimensional channel estimator is then enhanced with the aid of a time-domain predictor described in details in [1]. Our simulation results are presented in Section IV.

II. SYSTEM MODEL

The discrete baseband model of the OFDM/MC-CDMA system can be described as in [3]

$$y[n, k] = H[n, k]x[n, k] + w[n, k], \qquad (1)$$

for $k = 0, \ldots, K - 1$ and all n, where $y[n, k]$, $x[n, k]$ and $w[n, k]$ are the received symbol, the transmitted symbol and the Gaussian noise sample respectively, corresponding to the kth subcarrier of the nth OFDM block. Furthermore, $H[n, k]$ is the complex channel transfer function (CTF) coefficient associated with kth subcarrier and time instance n. Note, that in the case of an M-QAM modulated OFDM system, $x[n, k]$ corresponds to the M-QAM symbol accommodated by the kth subcarrier, while in a MC-CDMA system, such as a Walsh-Hadamard Transform (WHT) assisted OFDM scheme supporting G users [1] we have

$$x[n, k] = \sum_{p=0}^{G-1} c[k, p]s[n, p], \qquad (2)$$

where $c[k, p]$ is the kth chip of the pth spreading code, while $s[n, p]$ is the M-QAM symbol spread by the pth code. Each of the G spreading codes is constituted by G chips.

We now continue our discourse with a brief analysis of the properties of the channel model considered based on the widely used physical interpretation of the wireless mobile channel.

A. Channel Statistics

A Single Input Single Output (SISO) wireless communication link is constituted by a multiplicity of statistically independent components, termed as *paths*. Thus, such a channel is referred to as a *multipath* channel. The physical interpretation of each individual path is a single distortionless ray between the transmitter and the receiver antennas. We adopt the complex baseband representation of the continuous-time channel impulse response (CIR), as given by [4]

$$h(t, \tau) = \sum_{l} \alpha_l(t)c(\tau - \tau_l), \qquad (3)$$

where $\alpha_l(t)$ is the time-variant complex amplitude of the lth path and the τ_l is the corresponding path delay, while $c(\tau)$ is the aggregate impulse response of the transmitter-receiver pair, which usually corresponds to that of the raised-cosine Nyquist filter.

The scattered and delayed indirect signal paths usually arise as a result of diffraction from scattering surfaces and are termed as Non-Line-Of-Sight (NLOS) paths. In most recently proposed wireless mobile channel models each CIR component α_l associated with a NLOS channel path is modelled by a wide sense stationary (WSS) narrow-band complex Gaussian process [4] having correlation properties characterised by the cross-correlation function

$$E\{\alpha_i[n]\alpha_j^*[n - m]\} = r_t[m]\delta[i - j], \qquad (4)$$

where n is a discrete time-domain index and $\delta[\cdot]$ is the Kronecker delta function. The above equation suggests that the different CIR components are assumed to be mutually uncorrelated and each exhibits similar time-domain autocorrelation properties defined by the time-domain correlation function $r_t[n]$. The Fourier transform pair of the correlation function $r_t[n]$ associated with each CIR tap corresponds to a band-limited power spectral density (PSD) $p_t(f)$, such that we have $p_t(f) = 0$, if $|f| > f_d$, where f_d is termed as the *maximum Doppler frequency*. The time period $1/f_d$ is the so-called *coherence time* of the channel [4] and usually we have $1/f_d \gg T$, where T is the duration of the OFDM block $x[n]$.

A particularly popular model of the time-domain correlation function $r_t[n]$ was proposed by Jakes in [5] and is described by

$$r_t[n] \triangleq r_J[n] = J_0(nw_d), \qquad (5)$$

where $J_0(x)$ is a zero-order Bessel function of the first kind and $w_d = 2\pi T f_d$ is the normalised Doppler frequency. The corresponding U-shaped PSD function, termed as the Jakes-spectrum is given by [5]

$$p_J(w) = \begin{cases} \frac{2}{w_d} \frac{1}{\sqrt{1 - (w/w_d)^2}}, & \text{if } |w| < w_d \\ 0, & \text{otherwise.} \end{cases}$$

From (3) the continuous channel transfer function can be described as in [3]

$$
\begin{aligned}
H(t,f) &= \int_0^\infty h(t,\tau)\, e^{-j2\pi f\tau} d\tau \\
&= C(f) \sum_l \alpha_l(t)\, e^{-j2\pi f\tau_l}, \quad (6)
\end{aligned}
$$

where $C(f)$ is the Fourier transform pair of the transceiver's impulse response $c(\tau)$.

As it was pointed out in [6], in OFDM/MC-CDMA systems using a sufficiently long cyclic prefix and adequate synchronisation, the discrete CTF can be expressed as

$$
\begin{aligned}
H[n,k] &\triangleq H(nT, k\Delta f) \\
&= \sum_{m=0}^{K_0-1} W_K^{km} h[n,m] \\
&= C[k] \sum_{l=1}^{L} W_K^{k\tau_l/T_s} \alpha_l[n], \quad (7)
\end{aligned}
$$

for $k = -\frac{K}{2}, \cdots, \frac{K}{2} - 1$, where $h[n,m] \triangleq h(nT, mT/K)$ is the sample-spaced CIR (SS-CIR) and $W_K = \exp(-j2\pi/K)$. Note, that in realistic channel conditions associated with non-sample-spaced path-delays the receiver will encounter dispersed received signal components in several neighbouring samples owing to the convolution of the transmitted signal with the system's impulse response, which we refer to as leakage. This phenomenon is usually unavoidable and therefore the resultant SS-CIR $h[n,m]$ will be constituted of numerous correlated non-zero taps. By contrast, the fractionally-spaced CIR (FS-CIR) $\alpha_l[n] \triangleq \alpha_l(nT)$ will be constituted by a lower number of $L \ll K_0 \ll K$ non-zero statistically independent taps associated with distinctive propagation paths.
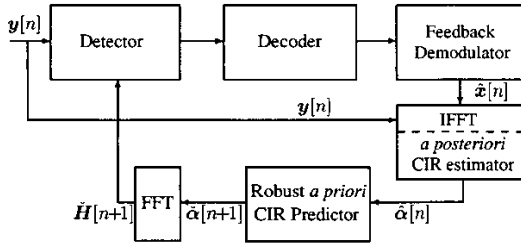
III. CHANNEL ESTIMATION

Fig. 1. Channel estimator constituted by an *a posteriori* decision-directed CIR estimator, based on frequency-domain modulated symbol estimates, followed by an *a priori* CIR predictor.

The schematics of the proposed channel estimation method is depicted in Figure 1. Our channel estimator is constituted by what we refer to as an *a posteriori* decision-directed CIR estimator followed by an *a priori* CIR predictor [1]. As seen in Figure 1, the task of the CIR estimator is to estimate the FS-CIR taps of Equation (7). The transformation from the subcarrier-related frequency domain to the FS-CIR-related time domain is invoked in order to exploit the frequency-domain correlation of the subcarrier-related CTF coefficients as well as to reduce the computational complexity associated with the CTF prediction process, because the FS-CIR typically has a lower number of $L \ll K$ significant taps, which have to be predicted, than the K number of FD-CTF coefficients. Hence the overall channel estimation complexity is reduced, even when the complexity of the FD-CTF to CIR transformation and its inverse are taken into account.

The *a posteriori* FS-CIR estimator inputs are the frequency-domain signal $y[n]$ and the decision-based estimate $\hat{x}[n]$. The transformation from the frequency to time domain is performed within the CIR estimator of Figure 1 and its output is an *a posteriori* estimate $\hat{\alpha}_l[n]$ of the FS-CIR taps of Equation (3) which is fed into the low-rank time-domain FS-CIR tap predictor of Figure 1 for the sake of producing an *a priori* estimate $\check{\alpha}[n+1, l]$ of the next FS-CIR on a FS-CIR tap-by-tap basis [1]. Finally, the predicted FS-CIR is converted to the FD-CTF. The resultant FD-CTF is employed by the receiver for the sake of detecting and decoding of the next OFDM symbol. Note, that this principle requires the transmission of a channel sounding sequence during the initialisation stage.

A. A Posteriori FS-CIR Estimator

We would like to commence our portrayal of the proposed channel estimation philosophy with the derivation of the *a posteriori* FS-CIR estimator of Figure 1.

By substituting the FD-CTF of Equation (7) into (1) we arrive at

$$
y[n,k] = C[k] \sum_{l=1}^{L} W_K^{k\frac{\tau_l}{T_s}} \alpha_l[n]\hat{x}[n,k] + w[n,k], \quad (8)
$$

which can be expressed in a matrix form as

$$
y[n] = \mathrm{diag}\,(C[k]\hat{x}[n,k])\, W\, \alpha[n] + w[n], \quad (9)
$$

where we define the $(K \times K)$-dimensional matrix $\mathrm{diag}\,(v[k])$ as a diagonal matrix with the corresponding elements of the vector $v[k]$ on the main diagonal, as well as the $(K \times L)$-dimensional Fourier Transform matrix W described by $W_{kl} \triangleq W_K^{k\frac{\tau_l}{T_s}}$ for $k = -\frac{K}{2}, \cdots, \frac{K}{2} - 1$ and $l = 1, \cdots, L$.

The MMSE estimator of the FS-CIR taps $\alpha_l[n]$ of the linear vector model described by (9) is given by [7]

$$
\begin{aligned}
\hat{\alpha} &= \left(C_\alpha^{-1} + \frac{1}{\sigma_w^2} W^H \mathrm{diag}\,\left(|C[k]\hat{x}[k]|^2\right) W \right)^{-1} \\
&\quad \times\; W^H \mathrm{diag}\,(C^*[k]\hat{x}^*[k])\, y, \quad (10)
\end{aligned}
$$

where we omit the time-domain OFDM-block-spaced index n for the sake of notational simplicity and define C_α as the covariance matrix of the FS-CIR vector α.

In order to characterise the properties of the expression (10) we would like to recall the corresponding properties of the matrices involved. The vector $C[k]$ is the discrete frequency response of the system's Nyquist filter $c(\tau)$ in Equation (3). It is evident that in any reasonably designed system, we have $|C(f)|^2 \approx 1$ for any values of f within the system's transmission band, which corresponds to $|C[k]|^2 \approx 1$ for $k = -\frac{K}{2}, \cdots, \frac{K}{2} - 1$, and therefore we have $\mathrm{diag}\,(C[k]) \approx I$. Furthermore, the matrix W is a Fourier Transform matrix having elements given by $W[k,l] = \exp -j2\pi \frac{k}{K}\frac{\tau_l}{T_s}$. Thus, the square matrix $W^H \mathrm{diag}\,(|\hat{x}[k]|^2)\, W$ is a Toeplitz Hermitian matrix.

Let us also recall that the channel model assumed is not limited by the Wide Sense Stationary (WSS) conditions. Thus the corresponding channel parameters σ_l^2 are time-variant and hence are characterised by the energy expectation value $\sigma_l^2 \triangleq E\left\{|\alpha_l[n]|^2\right\}$ of the FS-CIR's lth tap. The best estimate of the expectation value σ_l^2 available in the context of our FS-CIR estimator is the *a priori* estimate $|\check{\alpha}_l[n]|^2$ generated by the FS-CIR predictor of Figure 1. By substituting the corresponding estimates of the expectation values of the FS-CIR taps' energy into Equation (10) we arrive at

$$
\begin{aligned}
\hat{\alpha} &= \left(\mathrm{diag}\left(\frac{1}{|\check{\alpha}_l[n]|^2}\right) + \frac{1}{\sigma_w^2} W^H \mathrm{diag}\,\left(|\hat{x}[k]|^2\right) W \right)^{-1} \\
&\quad \times\; W^H \mathrm{diag}\,(C^*[k]\hat{x}^*[k])\, y, \quad (11)
\end{aligned}
$$

where the matrix inversion operation is performed for the low-rank $(L \times L)$-dimensional matrix $\left(\text{diag}\left(\frac{1}{|\hat{\alpha}_l[n]|^2}\right) + \frac{1}{\sigma_w^2}\mathbf{W}^H\text{diag}\left(|\hat{x}[k]|^2\right)\mathbf{W}\right)$.

We now turn our attention to the problem of exploiting the time-domain correlation of the FS-CIR taps $\alpha_l[n]$.

B. Time-Domain Channel Predictor

Our aim is to predict the FS-CIR taps $\{\alpha_1[n+1], \cdots, \alpha_L[n+1, K_0-1]\}$ associated with the channel expected during the reception of the next OFDM symbol, given the history of the previous CIRs, namely the *a posteriori* estimates $\{\{\hat{\alpha}_l[n]\}, \{\hat{\alpha}_l[n-1]\}, \cdots\}$, $l = 1, \cdots, L$.

As portrayed in Section II, the lth CIR tap $\alpha_l[n]$ undergoes a narrow-band time-domain fading process characterised by its cross-correlation properties, which can be described by

$$E\{\alpha_l^*[n]\alpha_{l'}[n-m]\} = r_t[m]\delta[l-l'], \quad (12)$$

where $r_t[n]$ is the corresponding time-domain correlation function and $\delta[\cdot]$ is the Kronecker Delta function.

This narrow-band WSS process can be approximately modelled as a finite impulse response (FIR) auto-regressive process of the order N_{tap} [1]

$$\alpha_l[n+1] = \sum_{m=0}^{N_{tap}-1} q[m]\alpha_l[n-m] + v_l[n+1], \quad (13)$$

where $q[m]$ represents the autoregressive coefficients and $v_l[n]$ is the model noise.

Let us now define the column vectors

$$\begin{aligned}\boldsymbol{\alpha}_l[n] &\triangleq (\alpha_l[n], \alpha_l[n-1], \cdots, \alpha_l[n-N_{tap}+1])^T \\ \boldsymbol{q} &\triangleq (q[0], 1[1], \cdots, q[N_{tap}-1])^T \end{aligned} \quad (14)$$

and rewrite Equation (13) in a vectorial form as

$$\alpha_l[n+1] = \boldsymbol{\alpha}_l[n]^T\boldsymbol{q} + v[n+1]. \quad (15)$$

Left-multiplying both sides of (15) with the complex conjugate of the column vector $\boldsymbol{\alpha}_l[n, l]$ and obtaining the expectation value over the time-domain index n yields

$$E\{\boldsymbol{\alpha}_l^*[n]\alpha_l[n+1]\} = E\{\boldsymbol{\alpha}_l^*[n](\boldsymbol{\alpha}_l^T[n]\boldsymbol{q} + v[n+1])\}, \quad (16)$$

which can be represented as a set of Yule-Walker or Wiener-Hopf equations in the following form [8]

$$\boldsymbol{r}_{apr} = \boldsymbol{R}_{apt}\boldsymbol{q}, \quad (17)$$

where the vector $\boldsymbol{r}_{apr}$ is the autocorrelation vector of the predicted *a priori* CIR taps defined by

$$\boldsymbol{r}_{apr} = \frac{1}{\sigma_l^2}E\{\boldsymbol{\alpha}_l^*[n]\alpha_l[n+1]\}, \quad (18)$$

and the matrix $\boldsymbol{R}_{apt}$ is the autocorrelation matrix of the *a posteriori* CIR taps described in [1]

$$\begin{aligned}\boldsymbol{R}_{apt} &= \frac{1}{\sigma_l^2}E\{\hat{\boldsymbol{\alpha}}_l[n]\hat{\boldsymbol{\alpha}}_l^H[n]\} \\ &= \boldsymbol{R}_{apr} + \rho\boldsymbol{I}, \\ \text{where} \quad \boldsymbol{R}_{apr} &= \frac{1}{\sigma_l^2}E\{\boldsymbol{\alpha}_l[n]\boldsymbol{\alpha}_l^H[n]\}. \end{aligned} \quad (19)$$

The optimal solution of Equation (17) evaluated in the MSE sense is given by

$$\boldsymbol{q}_{pre} = \boldsymbol{R}_{apt}^{-1}\boldsymbol{r}_{apr}. \quad (20)$$

In the specific scenario when the channel is described by Jakes' model [5], the *a priori* autocorrelation vector $\boldsymbol{r}_{apr}$ can be formulated as $r_{apr}[n] = r_J[n] = J_0(2\pi F_d n)$, $n = 1, 2, \ldots, N_{tap}$, where $J_0(x)$ is a zero-order Bessel function of the first kind. The corresponding *a posteriori* autocorrelation matrix $\boldsymbol{R}_{apr}$ is given by $R_{apr}[n, m] = r_J[n-m] + \rho\delta[n-m]$, $n, m = 0, 1, \ldots N_{tap} - 1$, while the CIR predictor's coefficient vector is described by (20) and the prediction is performed according to

$$\check{\alpha}_l[n+1] = \boldsymbol{q}_{pre}^T\hat{\boldsymbol{\alpha}}_l[n], \quad l = 1, 2, \ldots, L. \quad (21)$$

C. Robust Predictor

The CIR-tap prediction process described in the previous subsection exhibits a high CIR-tap estimation performance under the assumption of having perfect knowledge of the channel statistics. However, it suffers from a significant performance degradation, when the actual channel statistics deviate from the model assumed, such as for example Jakes' model. The issue of statistical mismatch becomes increasingly detrimental in diverse wireless environments, where the channel conditions and the corresponding statistics are time-dependent and cannot be assumed to be wide-sense stationary.

As it has been shown in [6] and [1], the MSE of the linear CIR predictor of (21) is upper-bounded by the MSE encountered, when communicating over an ideally band-limited channel having a perfect low-pass Doppler PSD function given by

$$p_{B,unif}(f) = \begin{cases} \frac{1}{2f_d}, & \text{if } |f| < f_d \\ 0, & \text{otherwise}. \end{cases} \quad (22)$$

Hence, we arrive at the concept of designing Li's [6] so-called *robust* linear predictor [1], which assumes encountering the worst possible channel statistics. As pointed out in [9], such a *robust* channel predictor, optimised for the worst-case PSD of Equation (22), can be designed by using the corresponding sinc-shaped *a priori* autocorrelation vector $\boldsymbol{r}_{apr,rob}$, which is given by

$$r_{apr,rob}[n] = r_B[n] = \frac{\sin 2\pi f_d n}{2\pi f_d n}, \quad n = 1, 2, \ldots, N_{tap} \quad (23)$$

and by invoking the corresponding *a posteriori* autocorrelation matrix $\boldsymbol{R}_{apt,rob}$ defined by

$$R_{apr,rob}[n, m] = r_B[n-m] + \rho\delta[n-m], \quad (24)$$

where we have $n, m = 0, 1, \ldots N_{tap} - 1$. The robust time-domain *a priori* FS-CIR tap predictor employed in the channel estimation scheme depicted in Figure 1 is extensively characterised in [1].

D. Complexity Study

The complexity of the proposed CIR estimation method of Figure 1 was found to be lower than that of other channel estimation techniques of comparable performance, such as that of the estimators proposed and investigated in [6] and [1]. More explicitly, the *a posteriori* estimator of Equation (10) has a computational complexity which is of the order of $O(L^2K + L^3)$, where L is the number of significant FS-CIR taps encountered and K is the number of OFDM subcarriers.

The robust CIR predictor [1] requires N_{tap} number of complex multiplications per CIR tap. In the specific scenario, where the channel's multipath intensity profile (MIP) is known, the actual prediction is performed only for a small number of significant FS-CIR taps. By contrast, when no channel statistics information is available, a larger number of CIR taps can be predicted. The insignificant CIR taps can then be discarded by assigning a zero value to them for the sake of mitigating the effects of the channel estimation noise encountered.

IV. SIMULATION RESULTS

In this section, we present our simulation results for the CIR estimation scheme advocated both in the context of OFDM and MC-CDMA systems communicating over multi-path Rayleigh fading channels.

A. System Parameters

TABLE I
SYSTEM PARAMETERS.

Parameter	OFDM	MC-CDMA
Channel bandwidth	800 kHz	
Number of carriers K	128	
Symbol duration T	160 μs	
Max. delay spread τ_{max}	40 μs	
No. of CIR taps	3	
Channel interleaver	WCDMA [10] 248 bit	–
Modulation	QPSK	
Spreading scheme	–	WH
FEC component codes code interleaver	Turbo code [11] , rate 1/2 RSC, K=3(7,5) WCDMA (124 bit)	

Our simulations were performed in the base-band frequency domain and the system configuration characterised in Table I is to a large extent similar to that in [6]. We assume having a total bandwidth of 800kHz. In the OFDM mode, the system utilises 128 QPSK-modulated orthogonal subcarriers. In the MC-CDMA mode we employ a full set of 128-chip Walsh-Hadamard (WH) codes for frequency-domain spreading of the QPSK-modulated bits over 128 orthogonal subcarriers. All spreading codes are assigned to a single user and the data-rate is similar in both the OFDM and the MC-CDMA modes. For forward error correction (FEC) we use $\frac{1}{2}$-rate turbo coding [11] employing two constraint-length $K = 3$ Recursive Systematic Convolutional (RSC) component codes and a 124-bit WCDMA code interleaver [10]. The octally represented generator polynomials of (7,5) were used.

We employed a three-path Rayleigh-fading channel model associated with delay spreads of up to $\tau_{max} = 40\mu s$ and varied the Doppler frequency f_d in the range of $5 - 200$ Hz. Our simulations were performed for various types of multipath intensity profiles and it was found that the channel estimator's performance is lower-bounded by the uniform multipath intensity profile (see also [1]). Therefore, we consider the uniform intensity profile as the worst-case scenario and present our results for this scenario only.

The channel is assumed to be quasi-stationary, namely we assume the channel's CIR to be constant for the duration of one OFDM/MC-CDMA symbol and assume different tap values before the arrival of the next OFDM symbol. Furthermore, we assume having perfect power control, resulting in having a constant overall channel output energy, namely to

$$\sum_i |\alpha_l[n]|^2 = \frac{1}{K} \sum_{k=0}^{K-1} |H[n,k]|^2 = 1 \qquad (25)$$

for all n. The reason for stipulating this assumption was to avoid the situation, where the system's performance is dominated by the time-domain distribution of the overall power level of the received signal inflicted by the particular channel-model. [1]
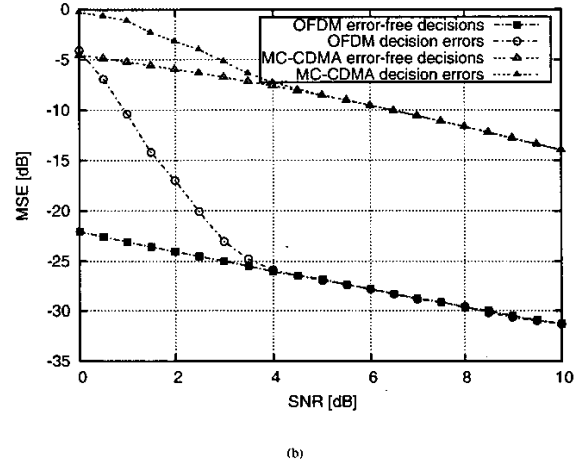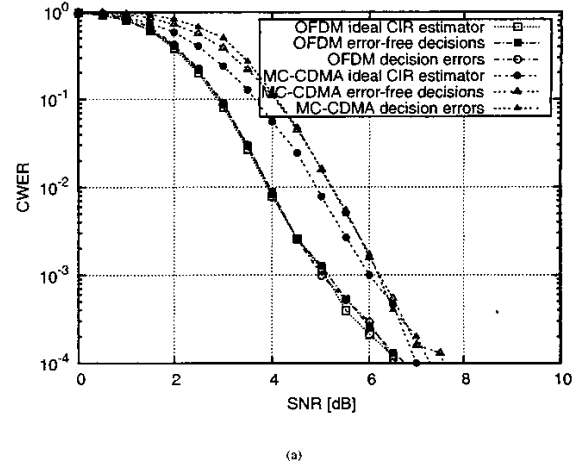

(a)

(b)

Fig. 2. (a) CWER and (b) MSE of the QPSK-modulated OFDM and MC-CDMA systems with DDCE and robust time-domain predictor under matched Doppler PSD conditions having a OFDM-symbol normalised Doppler frequency of $f_d T$ =0.01. We assume here having an infinite time-domain interleaver, which is equivalent to having a constant overall channel output energy.

B. Performance Results

Figure 2 demonstrates (a) the achievable turbo-coded Code-Word Error Rate (CWER), where a Code-Word corresponds to a single turbo-coded OFDM/MC-CDMA symbol, and (b) the MSE performance of the channel estimator for both the OFDM and the MC-CDMA systems considered under matched time-domain channel correlation conditions. Thus, the Doppler frequency assumed in the design of the robust CIR predictor matches the actual Doppler frequency of the Jakes-correlated Rayleigh fading channel. The channel estimator featured employs the a posteriori FS-CIR estimator of Section III-A followed by the robust a priori CIR predictor , as depicted in Figure 1. The simulations were carried out over the period of 100,000 QPSK-modulated $K = 128$-

[1]We note that in practice this condition cannot be maintained. However, this assumption allowed us to avoid that the performance be dominated by instances, when an OFDM symbol was received at a low power, which would obfuscate the most important performance trends.
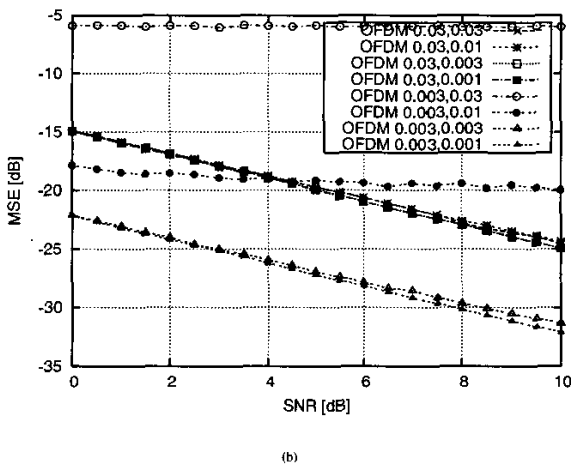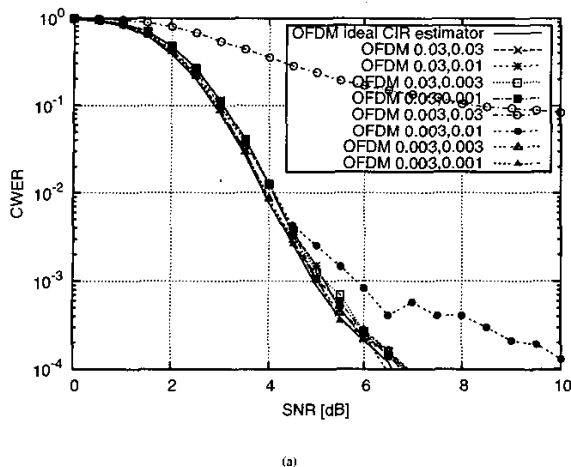
(a)

(b)

Fig. 3. (a) CWER and (b) MSE of the QPSK-modulated OFDM system with DDCE and robust time-domain predictor under unmatched Doppler PSD conditions having OFDM-symbol normalised Doppler frequencies of $\hat{f}_d T$ = 0.03 and 0.003 assumed during the design of the predictor, while the actual OFDM-symbol normalised Doppler frequencies encountered where $f_d T$ = 0.03, 0.01, 0.003 and 0.001. The "ideal CIR estimator" curve in plot (a) corresponds to the OFDM system performance under the assumption of perfect CIR knowledge.

edge. This degradation is inflicted mainly by the associated sub-optimal MMSE multi-code detection process [1]. The channel estimator imposes a further slight SNR degradation of about 0.3 dB on the MC-CDMA mode as a result of the Rayleigh-like energy distribution of the transmitted frequency-domain subcarriers $x[n, k]$ within each OFDM symbol, which are employed in the CIR estimator of Section III-A. By contrast, in the QPSK-modulated OFDM mode the energy of the transmitted frequency-domain samples $x[n, k]$ remains constant.

Finally, Figure 3 depicts (a) the CWER and (b) the MSE performance of the channel estimator in the context of an OFDM system under unmatched time-domain channel correlation conditions. Our simulations were performed for two different values of the OFDM-symbol normalised Doppler frequency assumed during the design of the robust CIR predictor, namely for $\hat{f}_d T$ = 0.03 and 0.003. Furthermore, four different values of the actual normalised Doppler frequencies were used, namely $f_d T$ = 0.03, 0.01, 0.003 and 0.001. It can be seen that the performance of the CIR predictor advocated is indeed tolerant to the mismatch of the actual Doppler frequency and that assumed during the predictor design, as long as the actual Doppler frequency does not exceed the value assumed in the predictor's design.

V. SUMMARY

In this paper we have proposed a channel estimation method, which is based on a low-complexity decision directed MMSE FS-CIR estimator combined with a robust time-domain FS-CIR predictor. We have found that the method proposed is effective in both WSS channels associated with a constant power intensity profile (PIP) and in channels having time-variant PIP. In the case of constant PIP the knowledge of the channel's correlation properties can be exploited by the receiver for increasing the accuracy of the channel estimation process.

REFERENCES

[1] L. Hanzo, Münster, B. Choi, and T. Keller, *OFDM and MC-CDMA for Broadband Multi-user Communications, WLANs and Broadcasting*. John Wiley – IEEE Press, 2003.

[2] A. Goldsmith, S. Jafar, N. Jindal, and S. Vishwanath, "Capacity limits of MIMO channels," *IEEE Journal on Selected Areas in Communications*, vol. 21, pp. 684–702, June 2003.

[3] Y. Li, "Simplified channel estimation for OFDM systems with multiple transmit antennas," *IEEE Transactions on Wireless Communications*, vol. 1, pp. 67–75, January 2002.

[4] R. Steele and L. Hanzo, eds., *Mobile Radio Communications*. New York, USA: IEEE Press - John Wiley & Sons, 2nd ed., 1999.

[5] W. Jakes Jr., ed., *Microwave Mobile Communications*. New York, USA: John Wiley & Sons, 1974.

[6] Y. Li, L. Cimini, and N. Sollenberger, "Robust channel estimation for OFDM systems with rapid dispersive fading channels," *IEEE Transactions on Communications*, vol. 46, pp. 902–915, April 1998.

[7] S. Kay, *Fundamentals of Statistical Signal Processing*. Englewood Cliffs, NJ, USA: Prentice-Hall, 1998.

[8] S. L. Marple, *Digital spectral analysis with applications*. Englewood Cliffs, NJ, USA: Prentice Hall, 1987.

[9] M. Münster, *Antenna Diversity-Assisted Adaptive Wireless Multiuser OFDM Systems*. PhD thesis, University of Southampton, UK, 2002.

[10] H. Holma and A. Toskala, eds., *WCDMA for UMTS : Radio Access for Third Generation Mobile Communications*. John Wiley and Sons, Ltd., 2000.

[11] L. Hanzo, T. Liew, and B. Yeap, *Turbo Coding, Turbo Equalisation and Space-Time Coding*. John Wiley, IEEE Press, 2002. (For detailed contents, please refer to http://www-mobile.ecs.soton.ac.uk.).

subcarrier OFDM/MC-CDMA symbols. It can be seen in Figure 2(a), that the performance of the channel estimator evaluated in the OFDM mode is close to that of the ideal estimator assuming perfect knowledge of the CIR. More explicitly, at low SNR values the achievable performance is degraded by the associated decision-error propagation, however the decision process becomes reliable for SNRs in excess of 4 dB.

In the MC-CDMA mode a 128-chip WH spreading code was assumed and a single user transmitted all the spreading codes in parallel in order to maintain a data-rate similar to that of the OFDM system. All transmitted codes experienced the same SNR value. As seen in Figure 2, the MC-CDMA mode suffers from an SNR performance degradation of about 1 dB even under the assumption of a perfect CIR knowl-